Rotation of the Earth: introduction

A rich and fascinating subject, $\exists$ numerous irregularities in $\oplus$'s rotation. convenient to divide into 3 categories:

1. changes in length of day (l.o.d.) due to internal causes and due to tidal friction of $☾$ and to lesser extent $\odot$.
2. precession: due to external torques, change in orientation of Ω axis in space.
3. wobble: wobbling of solid $\oplus$ about its rotation axis, due to internal causes.

Briefly examine nature, cause and measurement of each of these.

1. Changes in l.o.d.: a slowing down or speeding up of rate of rotation. Modern measurements compare star transit times with time measured by uniform clocks. Early astronomers (20th century) used pendulum clocks.

Prior to this ∃ observations based on <u>Ephemeris time</u>, this uses planetary motions to define a uniform time scale, can compare time based on ⊕ rotation with this.

~ 1950's <u>q</u>uartz crystal clocks came into use, tend to drift over periods of a few years.

Modern observations use atomic freq<u>u</u>ency standards (cesium beam clocks) which are drift free and accurate to 1 part in 10^{10}.

Timekeeping and astronomy done by several groups : NBS, US Navy, BIH in Paris.

Observations best presented in a <u>spectrum</u>, a <u>continuous</u> spectrum with a few <u>lines</u> superposed. Schematically looks like:

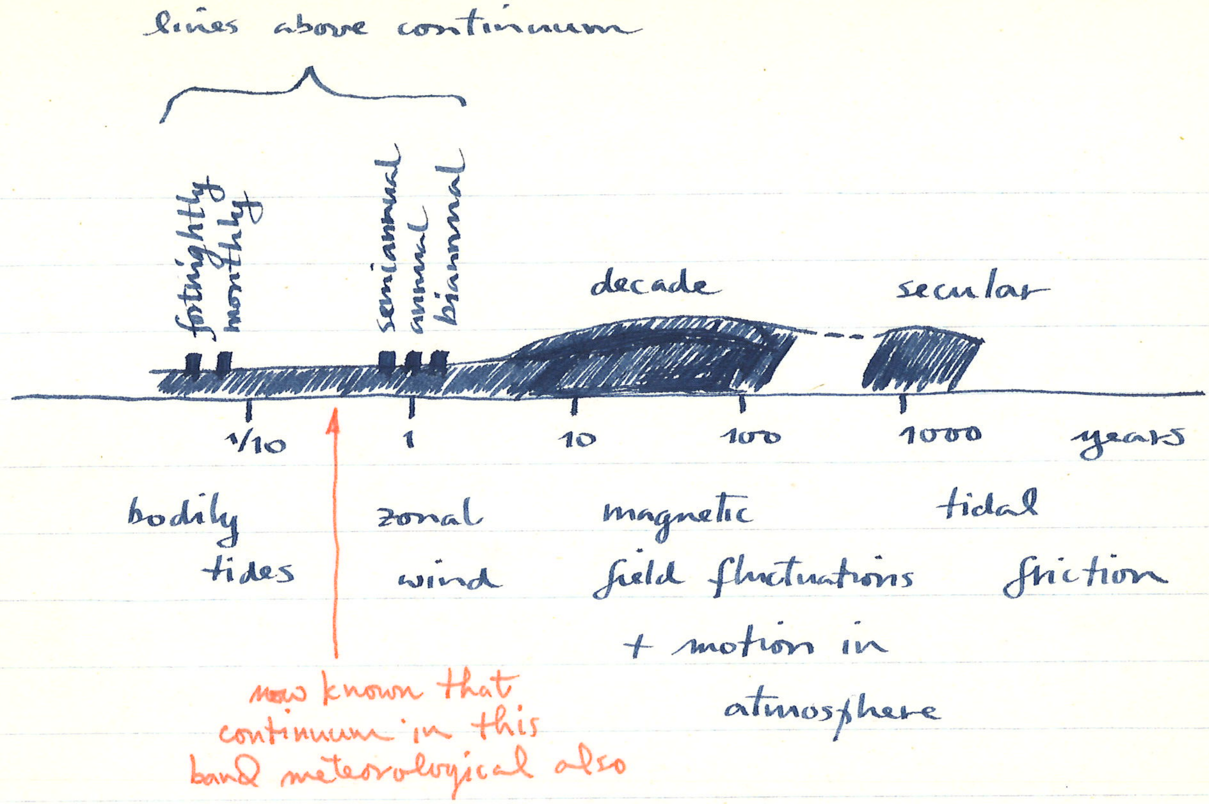

Two common ways of showing the data. Let $\bar{\Omega} \equiv$ <u>mean</u> rotation rate of $\oplus \equiv 7.292115 \cdot 10^{-5}$ rad/sec
Let $\Omega(t) \equiv$ <u>instantaneous</u> angular velocity of $\oplus$. The quantity often considered is then

$$m_3 \equiv (\Omega - \bar{\Omega}) / \bar{\Omega}$$
, the fractional change in angular velocity.

This is related to the change in the l.o.d. by

$$m_3 = - \Delta(\text{l.o.d.}) / \overline{\text{l.o.d.}}$$

The quantity actually observed is τ, the amount by which the $\oplus$ is slow after a time interval t, given by

$$m_3 = - d\tau / dt \quad \text{or}$$

$$\tau(t) = \tau(0) - \int_0^t m_3(t)\, dt$$

τ is an angle but measured in seconds.

The fortnightly, monthly and a fraction of the semiannual variations are due to bodily tides.

Tides deform solid $\oplus$, change principal moment of inertia C

Shape of long-period tides (only) is $P_2(\cos\theta)$ causes change in size of equatorial bulge.

$\underline{H} = C\underline{\omega_3}$ must remain constant (can change only by external torques

i.e. l.o.d. = 24 hours (1 ± 10^{-9})

Tidal changes in l.o.d. ~ 1 part in 10^{9} so τ is of order 0.1 to 0.2 msec (10^{-3} sec).

Fig. 5.7 of Lambeck shows time series of $m_3(t)$ for 1968 and Fig. 5.8 shows <u>spectrum</u> of same record. Peaks at 14 and 27 days, of right amplitude to be of tidal origin are visible.

Most of semi-annual and all of annual and biannual changes caused by seasonal fluctuations in <u>zonal</u> <u>winds</u> (winds which blow from E to W around the ⊕). These blow against mtns, bushes, buildings, etc. and exert torque on ⊕. Or, alternatively, can take point of view that $\underline{H}_{atm} + \underline{H}_{\oplus}$ must be conserved, if $\underline{H}_{atm}$ increases $\underline{H}_{\oplus}$ must decrease.

$\Delta(\text{l.o.d.}) \lesssim \pm 1\,\text{ms}$ in a year due to zonal winds

These are about 0.4 part in 10^8, so τ is of order 20–30 ms (longer than tidal changes since τ is cumulated amount ⊕ is slow).

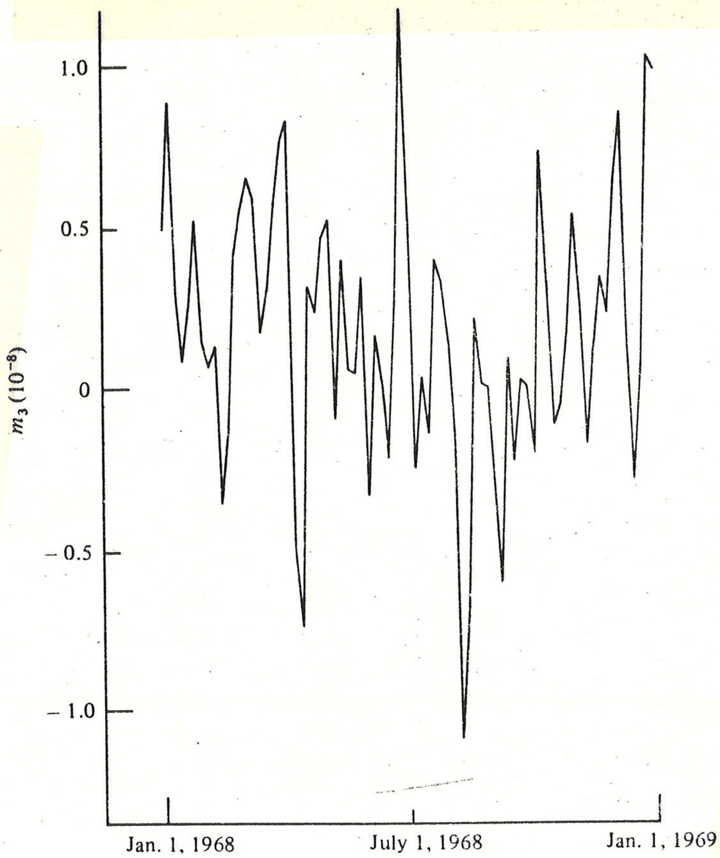

Figure 5.7. Time series of m_3 for 1968 based on the unsmoothed values of Π published by the BIH.

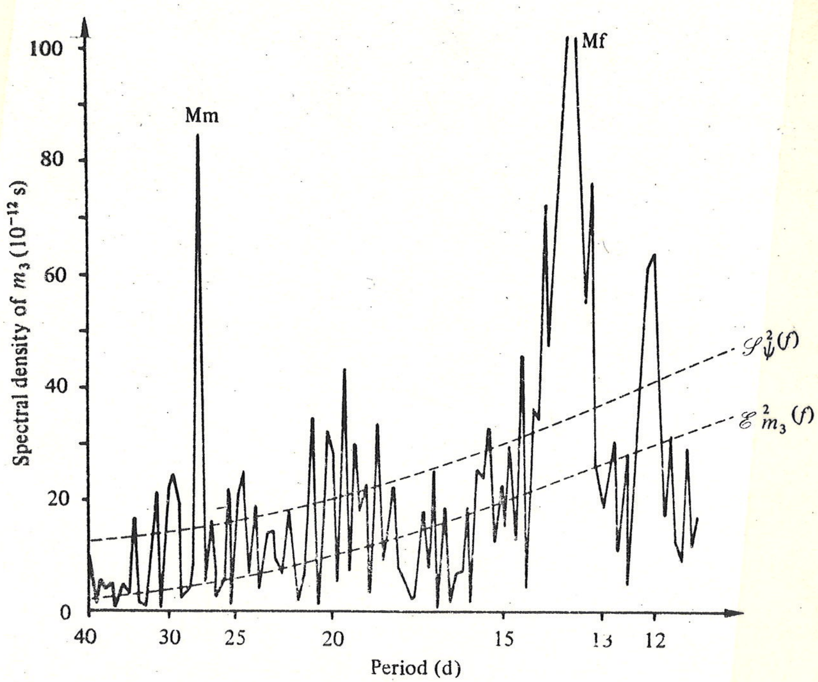

Figure 5.8. Unsmoothed amplitude spectrum of m_3. Tidal terms occur near 14 d (Mf) and near 27 d (Mm). The estimated error spectrum $\mathscr{E}_{m_3}(f)$ is based on $\nu_\Pi = 1$ ms. $\mathscr{S}_\psi(f)$ is the estimated continuum of the meteorological excitation spectrum.

Fig 5.6 of Lambeck shows $m_3(t)$ for period 1962 – 1978, annual and semiannual changes are apparent, Fig 1 from Lambeck + Cazenave shows spectrum of this data, peaks at 6 and 12 mo, plus energy at 2 – 3 yrs (quasi-biennial).

$\underline{H}_{atm}$ can be determined from measurements of wind velocity vs. altitude + latitude and compared with above.

Note effect of El Niño in mid 1982

Comparison for 1958 – 1962 shown Fig. 7.9 of Lambeck. Agreement excellent. Also recent evidence for good agreement with $\underline{H}_{atm}$ on shorter time scales (down to a few days). There are also irregular fluctuations with a time scale of decades. Most reliable determination since invention of crystal clocks 1955. Data after removal of annual + semi-annual lines shown Fig 5.5 of Lambeck, see fluctuations periods 6 – 8 years superposed on longer period (secular) changes.

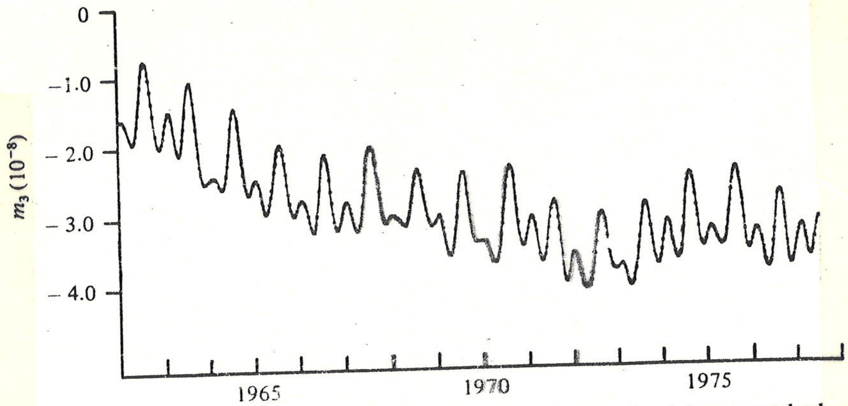

Figure 5.6. Time series of m_3 from 1962 to 1977 based on the smoothed values of Π published by the BIH.

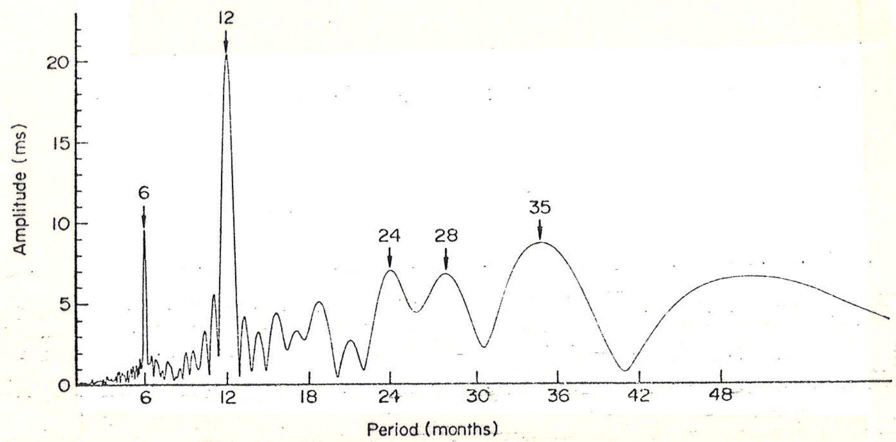

FIG. 3. Periodogram of the $-\tau$ after the elimination of the long-period variations.

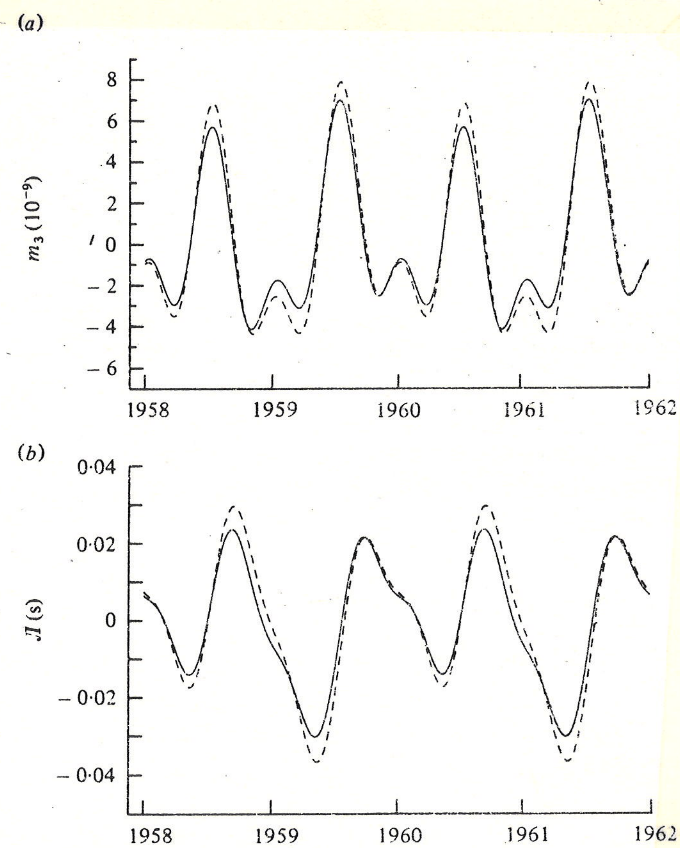

Figure 7.9. (*a*) Sum of the three seasonal excitation functions, compared with the astronomical estimate of m_3; (*b*) comparison of the meteorological and astronomic estimates of the seasonal amounts by which the Earth is slow. Astronomic estimates are indicated by broken curves.

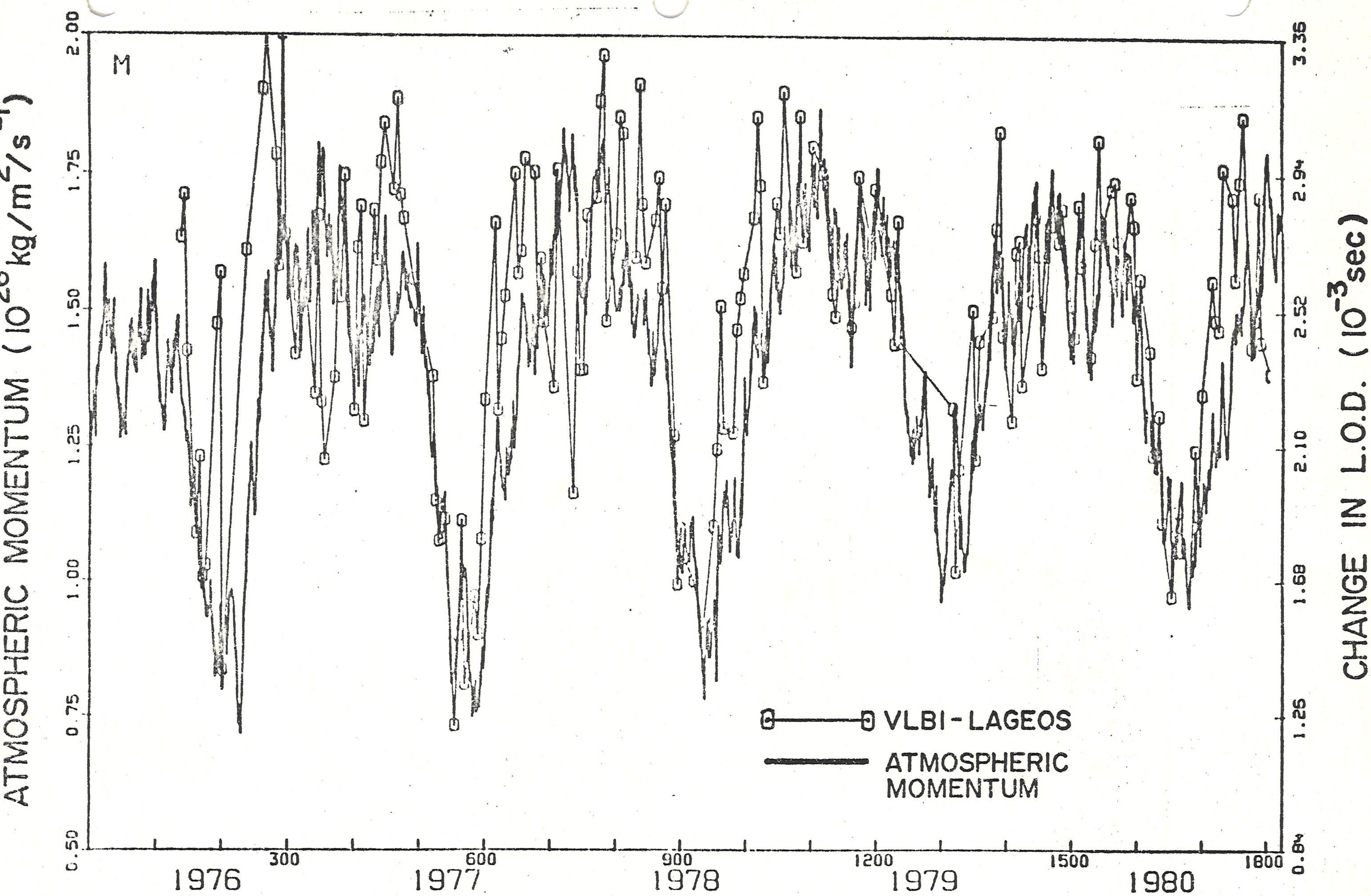
ATMOSPHERIC MOMENTUM (10^{26} kg/m²/s⁻¹)
CHANGE IN L.O.D. (10^{-3} sec)
M
2.00
1.75
1.50
1.25
1.00
0.75
0.50
3.36
2.94
2.52
2.10
1.68
1.26
0.84
300
600
900
1200
1500
1800
1976
1977
1978
1979
1980
VLBI - LAGEOS
ATMOSPHERIC MOMENTUM

Figure 4

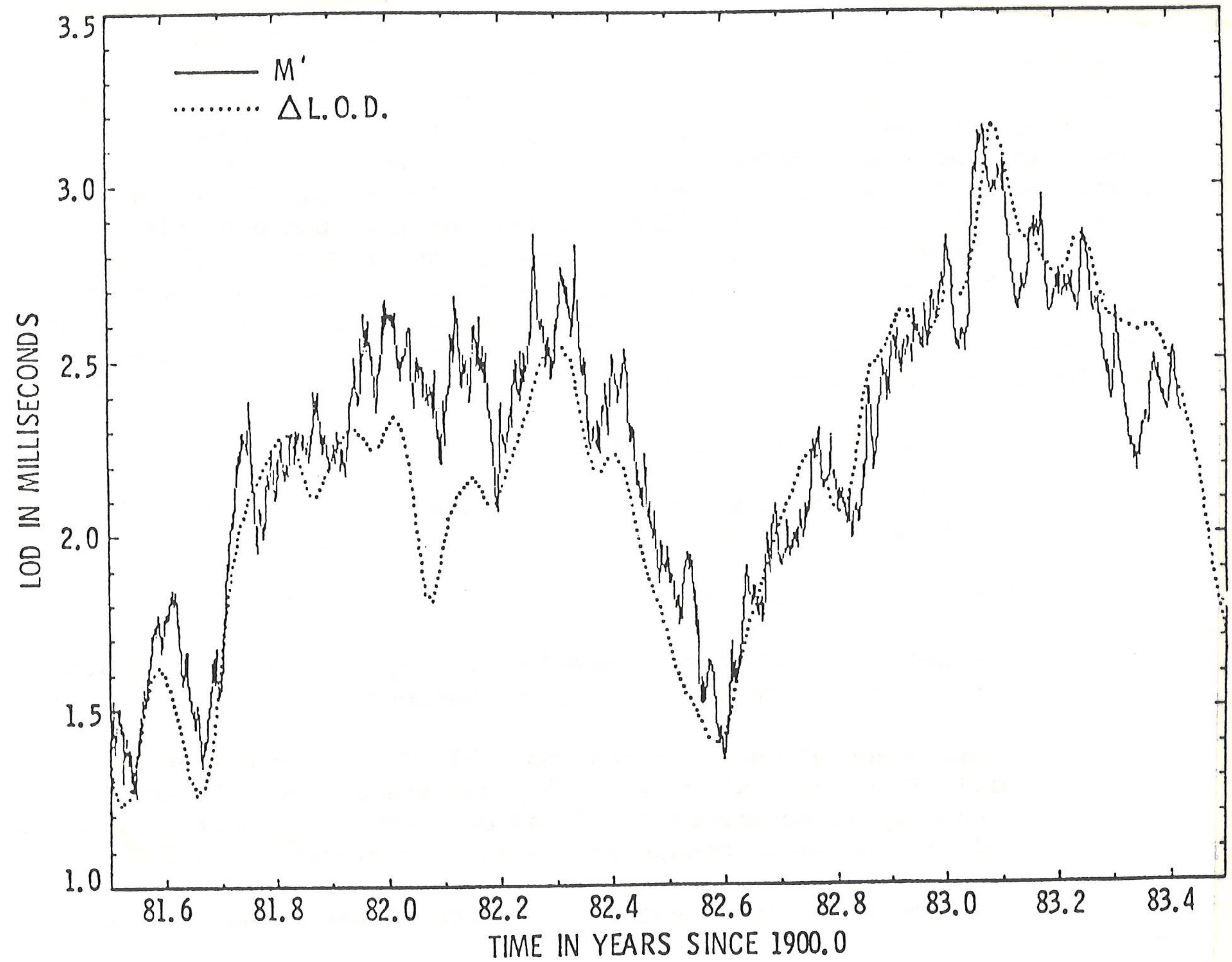

Figure 7. Change in Length of Day

Change in the length of day as determined from BIH data (dotted line) and as calculated on the basis of effects due to changes in the angular momentum of the atmosphere (solid line). (From Rosen, R. D., Salstein, D. A., Eubanks, T. M., Dickey, J. O., and Steppe, J. A. "An El Nino Signal in Atmospheric Angular Momentum and Earth Rotation," submitted to Science, February 1984).

Amplitudes few parts in 10^8.

Prior to 1955 data less reliable, based on comparisons with Ephemeris time.

$m_3(t)$ since 1820 as determined by independent analyses of Brouwer and Morrison Fig. 6 of Cazenave + Lambeck.

Variations, amplitude $\sim 5 \cdot 10^{-8}$, corresponds to Δ(l.o.d.) of a few (3–4 ms). The observed quantity τ is several tens of seconds because of the long period of the variations, this makes it possible to see sans clocks.

Some of this decade variation is probably due to decade climate variations, but principal cause thought to EM torques exerted on mantle by changing $\underline{B}(t)$ in core.

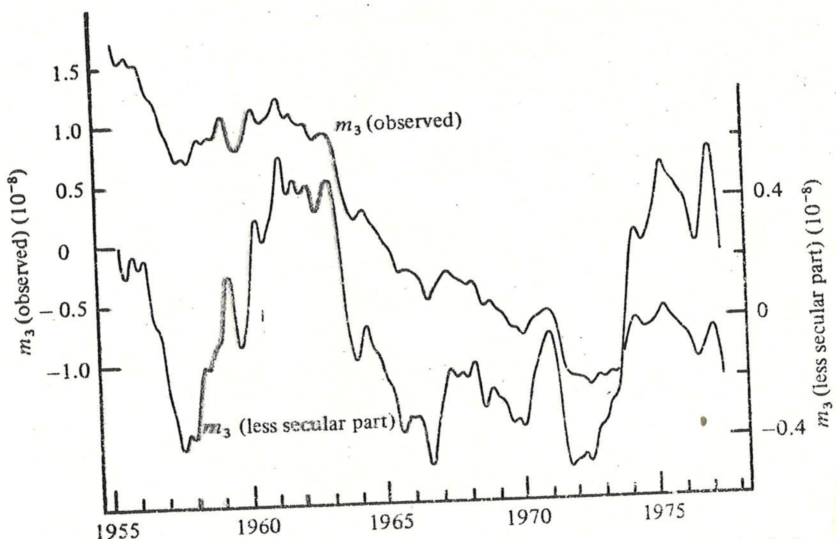

Figure 5.5. Time series of m_3 from 1955 to 1977 after removal of the 6-month and 12-month oscillations and after some smoothing to remove high-frequency (>6 cycle yr^{-1}) fluctuations.

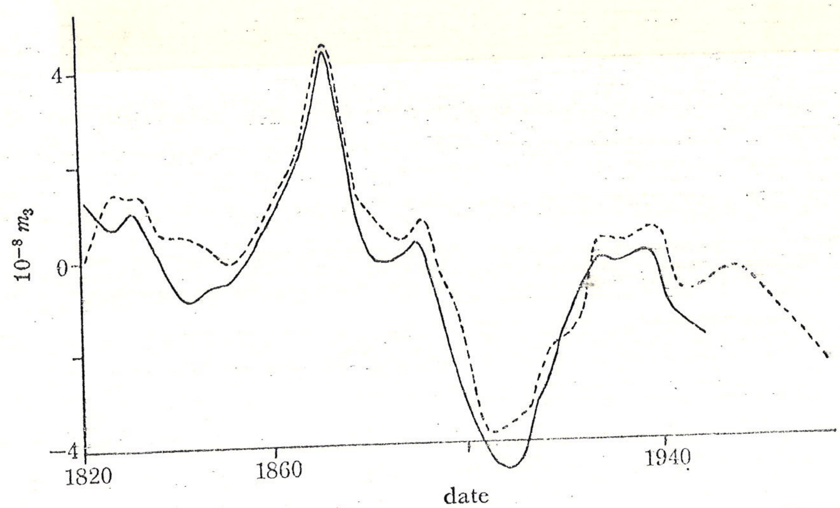

FIGURE 6. Long-period variations observed in m_3 since 1820 as determined by Brouwer (——) and by Morrison (– –).

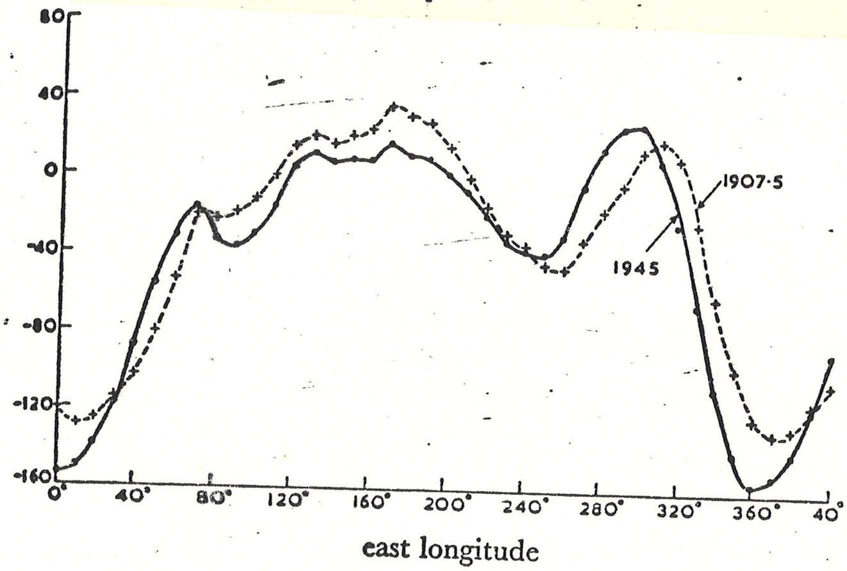

Figure 7. Vertical field on the equator.

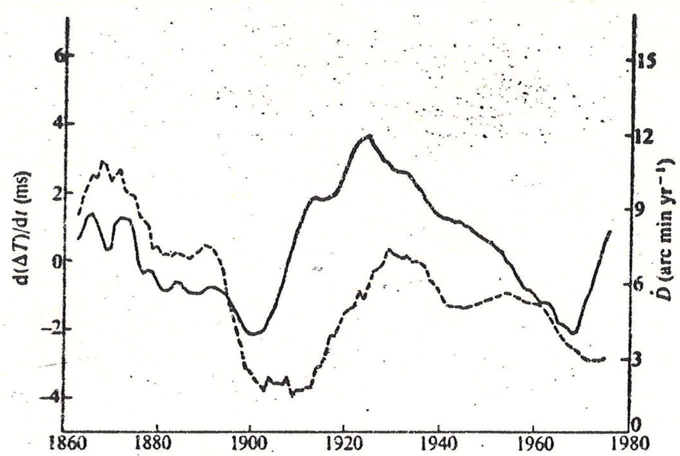

Fig. 1 Plot of the secular variation of declination $\dot{D}$ (solid curve and right hand scale) and of the excess length of day $d(\Delta T)/dt$ (dashed curve and left-hand scale) for the period 1861–1978. ΔT data are from refs. 18, 19. The relative changes in the Earth rotation rate $\Delta\Omega/\Omega$ are obtained from the $d(\Delta T)/dt$ values through multiplication by -1.157×10^{-8}.

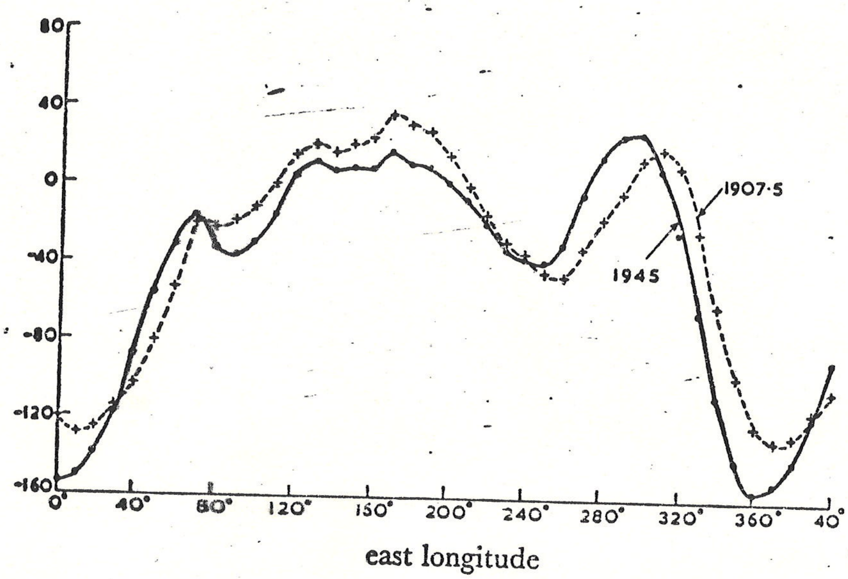

Figure 7. Vertical field on the equator.

westward drift of field ~ 0.2°/yr

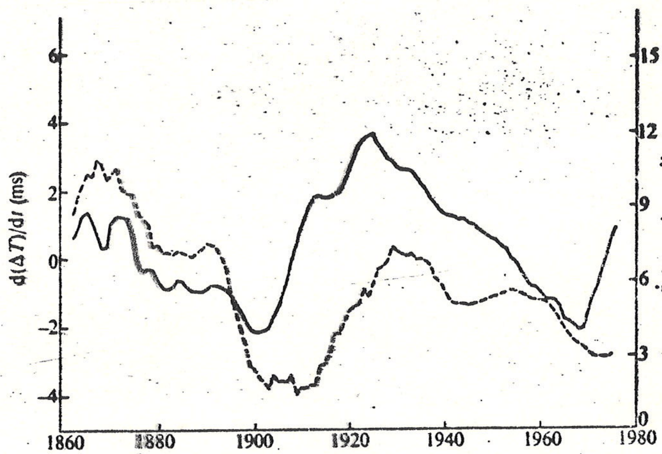

Fig. 1 Plot of the secular variation of declination $\dot{D}$ (solid curve and right hand scale) and of the excess length of day $d(\Delta T)/dt$ (dashed curve and left-hand scale) for the period 1861–1978. ΔT data are from refs. 18, 19. The relative changes in the Earth rotation rate $\Delta\Omega/\Omega$ are obtained from the $d(\Delta T)/dt$ values through multiplication by -1.157×10^{-8}.

last: note general slowing down trend since 1860; to find long time changes a new approach needed; study of ancient eclipses

magnetic variations lag behind spin variations because they must diffuse thru the mantle

declination : direction of compass needle

$\dot{D} \approx$ rate of westward drift of field

mantle spin follows average core; when upper part decelerates mantle accelerates ; fast westward drift (backward) correlated with fast spin

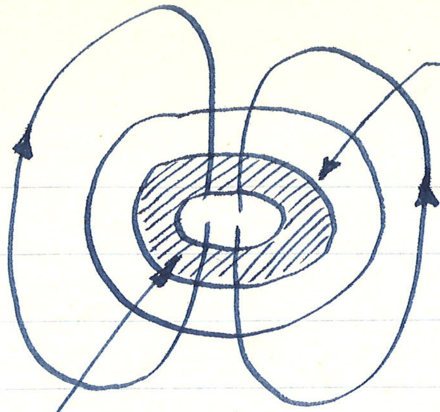

$\sigma \sim 10 - 100$ mho/m

$\sigma_{cu} = 10^8$ mho/m

$\sigma_{\text{distilled } H_2O} = 10^{-4}$ mho/m

Secular variation of $\underline{B}(t)$ on decade time scale induces currents in lower mantle; these interact (Lenz's law) to exert torques on mantle.

All the above changes produced by indigenous events. In all, $\underline{H}_{\oplus} = \underline{H}_{mantle} + \underline{H}_{core} + \underline{H}_{atm}$ is conserved.

There is also a steady slowing down of ⊕'s rotation due to tidal friction, an external influence. This secular change has been measured since ~ 1700. Without clocks by observing occultations of ☾, ☉ and ☿ Mercury. Also modern determinations using clocks and also satellite determinations of tidal bulge lag, also determined by lunar laser ranging. All agree that secular deceleration due to tidal friction (and other causes) is:

$$\dot{\Omega}_{total} \cong -5 \cdot 10^{-22} \ \text{rad}/\text{sec}^2$$

corresponds to 2.7 ms/century change in l.o.d.

τ however is substantial because of secularity – responsible for occasional leap seconds.

There also appears to be a slight secular acceleration due to internal causes, possibly response to deglaciation, so that $\dot{\Omega}_{total}$ is somewhat larger (more negative) than $\dot{\Omega}_{tidal}$. Telescope data covers too short an interval to get $\dot{\Omega}_{total}$ very accurately and ancient eclipse data is used, an interesting combination of astro-geophysics and classical studies.

$$\dot{\Omega}_{total} \sim -5 \cdot 10^{-22} \ \text{rad}/\text{s}^2$$
$$\dot{\Omega}_{tidal} \sim -7 \cdot 10^{-22} \ \text{rad}/\text{s}^2$$
$$\dot{\Omega}_{nontidal} \sim 1-2 \cdot 10^{22} \ \text{rad}/\text{s}^2$$

Both $\dot{\Omega}_{total}$ and $\dot{\Omega}_{tidal}$ known to only 10–20 % so $\dot{\Omega}_{nontidal}$ is of doubtful significance.

$\dot{\Omega}_{total}$ and $\dot{\Omega}_{tidal}$ can be separated because the latter affects the lunar orbit also, one observes <u>lunar occultations</u>.

Cause of <u>tidal</u> deceleration is torque exerted (mostly) by ☾ on lagged tidal bulge (first proposed 1754 by Kant to explain known lunar discrepancies)

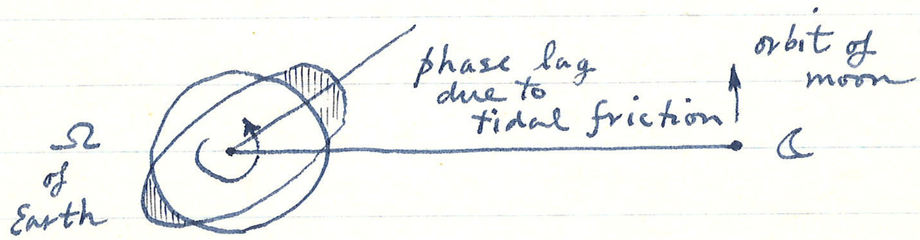

$\underline{H}_{\oplus}$ changes but $\underline{H}_{\oplus} + \underline{H}_{☾}$ (orbital) remains roughly constant (ignoring sun)
Rotation rate of ⊕ slows down and ☾ slows down in its orbit and moves away from ⊕ at a few cm/yr.

A fascinating problem: we'll discuss in more detail, many questions (where and how is energy dissipated, what is extrapolated past history of ⊕☾ system, can one extrapolate to future, etc?).

2. precession and forced nutation

A consequence of action of external torques on permanent bulge of ⊕, would occur in absence of friction. Principal phenomenon is precession of equinoxes but complex orbit of ☾ causes small nutations (nodding) to be superposed on this.

All these are motions of ⊕'s $\underline{H}$ vector in space (its orientation changes).

Largest or principal nutation has an amplitude of 8" of arc and a period 18.6 years

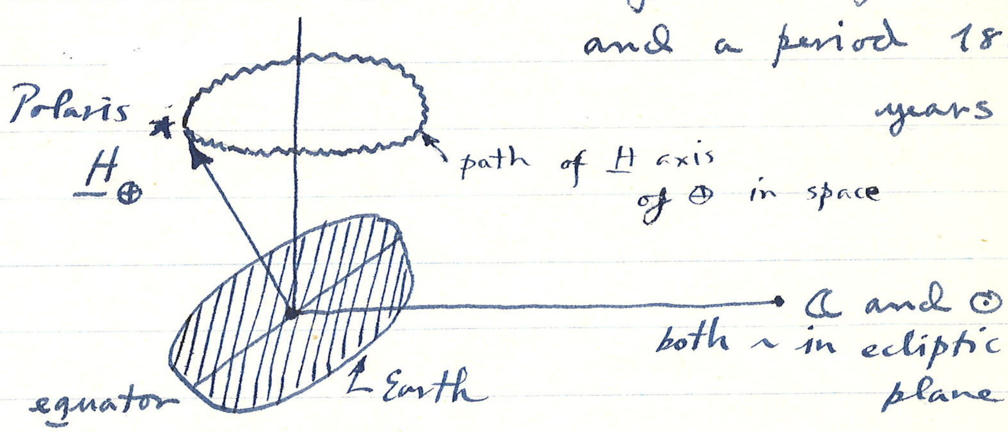

Precession period 25,800 years.
Next largest nutations semi-annual and fortnightly

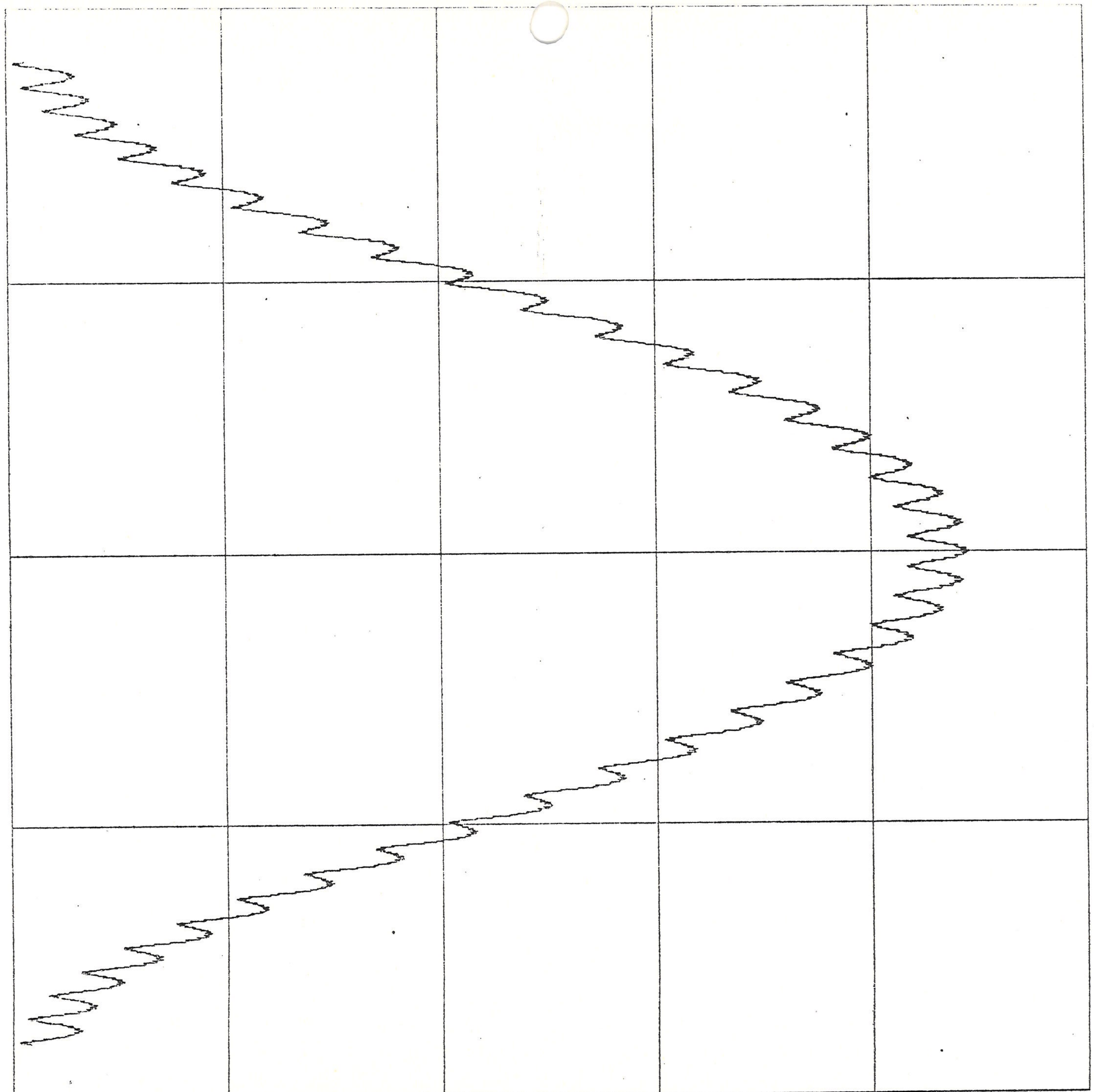

PRINCIPAL, SEMI-ANNUAL, AND FORT-NIGHTLY .39794 -x- .39804 -.001 -y- .001

Intimate connection of nutations with diurnal tides, no time to explore here but note that only diurnal tides exert net torque on ⊕

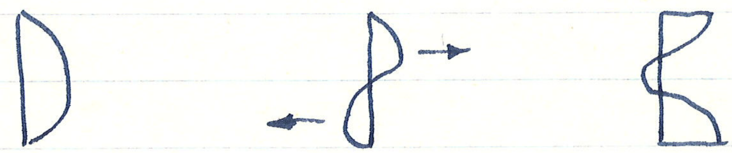

Path of $\underline{H}$ axis in 18.6 yrs from MLS.

3. wobble of ⊕ about its rotation axis

This due strictly to events on ⊕, not caused by external torques. To be distinguished from precession.

Wobble : $\underline{H}_{\oplus}$ is constant, ⊕'s principal axis of inertia displaced from rotation axis.

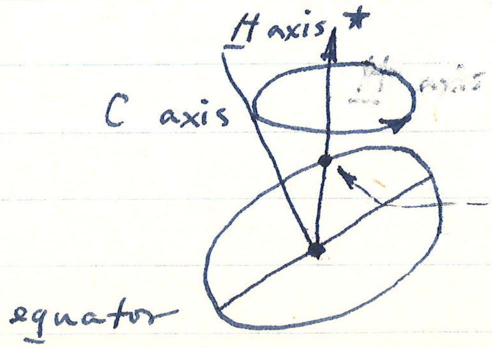

$\underline{H}$ and $\underline{\Omega}$ are (essentially) aligned

To an observer on ⊕, the rotation axis appears to move, wobble also called <u>polar motion</u>.

A way to measure polar motion + distinguish from precession, nutation, <u>in principle</u>.

Time exposure of star trails on a camera pointed straight up (<u>w.r.t.</u> <u>local vertical</u>). At one point on ⊕ surface center ★ in photo appears in center of photo itself.

star trails.

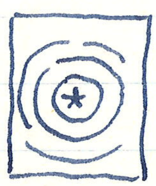

That point is where rotation axis of ⊕ skewers photographer. Up near N pole.

Point found to change slowly with time, this is wobble (★ in center is same)

Precession + nutation : the ★ changes.

Actual observations made using so-called PZT's (photographic <u>zenith</u> tubes) at many locations on ⊕'s surface.

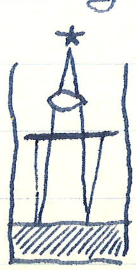

objective lens

photo plate

pool of liquid Hg reflecting mirror + define local vertical.

Best recent determinations from Doppler tracking of artificial satellites. See determinations from LAGEOS 1976 – 1980 and IRIS pole path '83 – '84.

See also 1974 comparison of LAGEOS and VLBI.

Fig. 5.10 of Lambeck shows path of pole determined by two organizations ILS and BIH for 1968 – 1970. Data noisier than optimistic "error bars" indicate.

Amplitude of motion

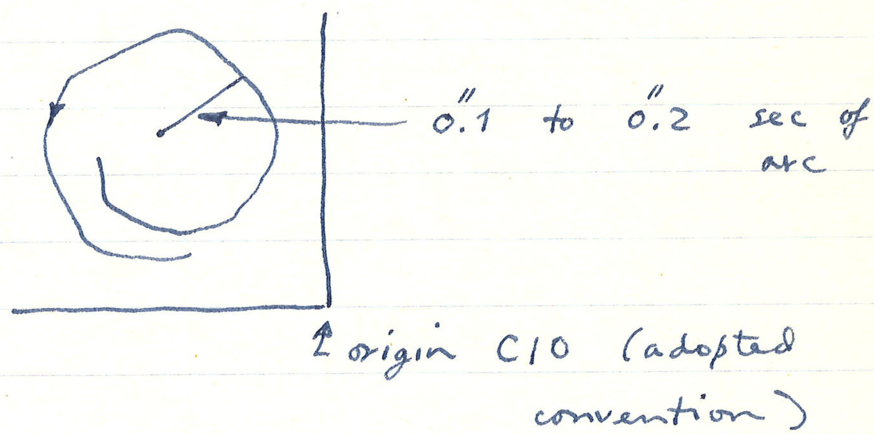

1 centisecond = 0.01″ ≈ 1 ft. subtended on ⊕'s surface so amplitude is 10 – 20 feet or 3 to 6 meters. Very small, hard to detect, obscured by atmospheric refraction effects, requires hundreds of observatories.

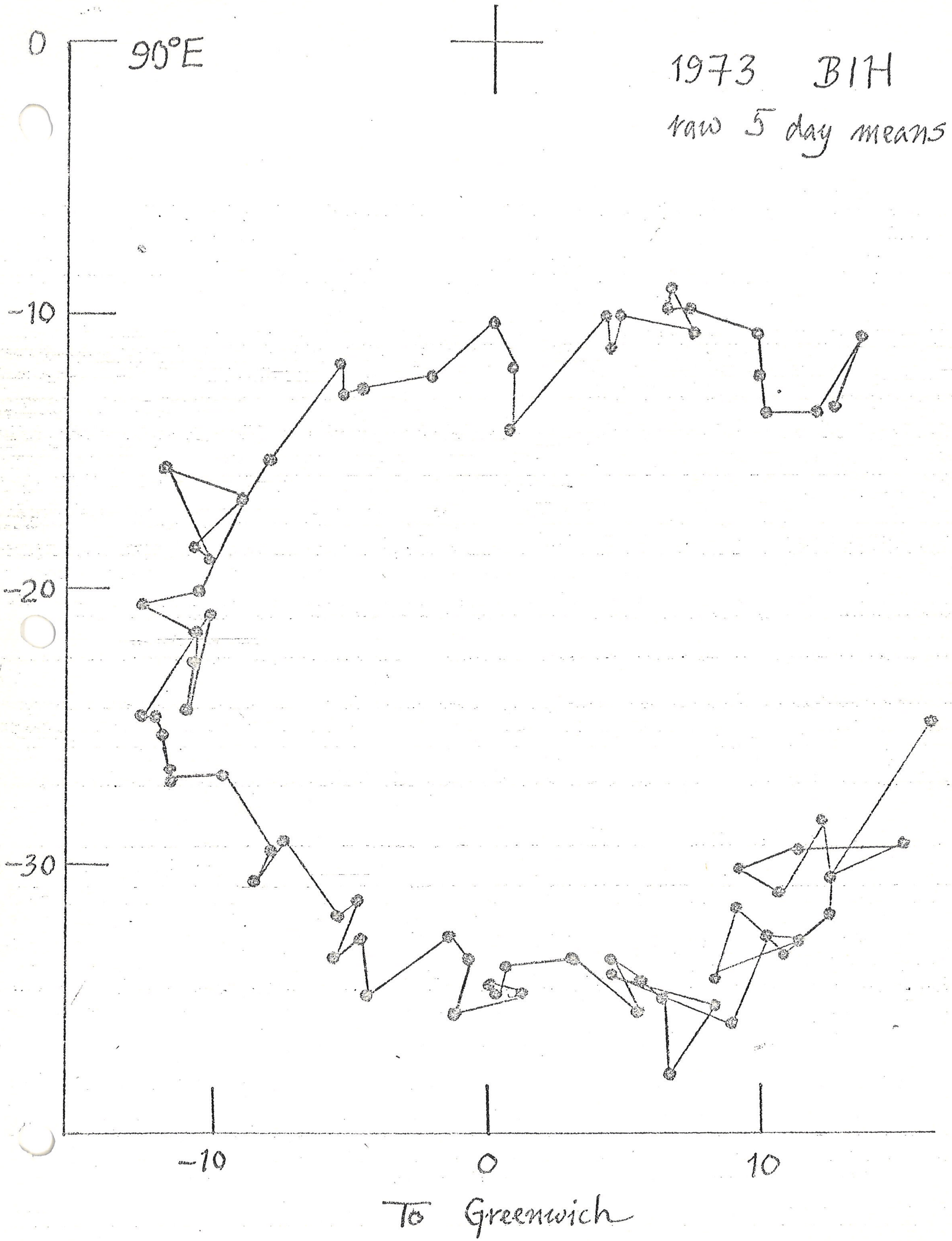

1973 BIH
raw 5 day means
90°E
0
-10
-20
-30
-10
0
10
To Greenwich

Polar motion determined by LAGEOS

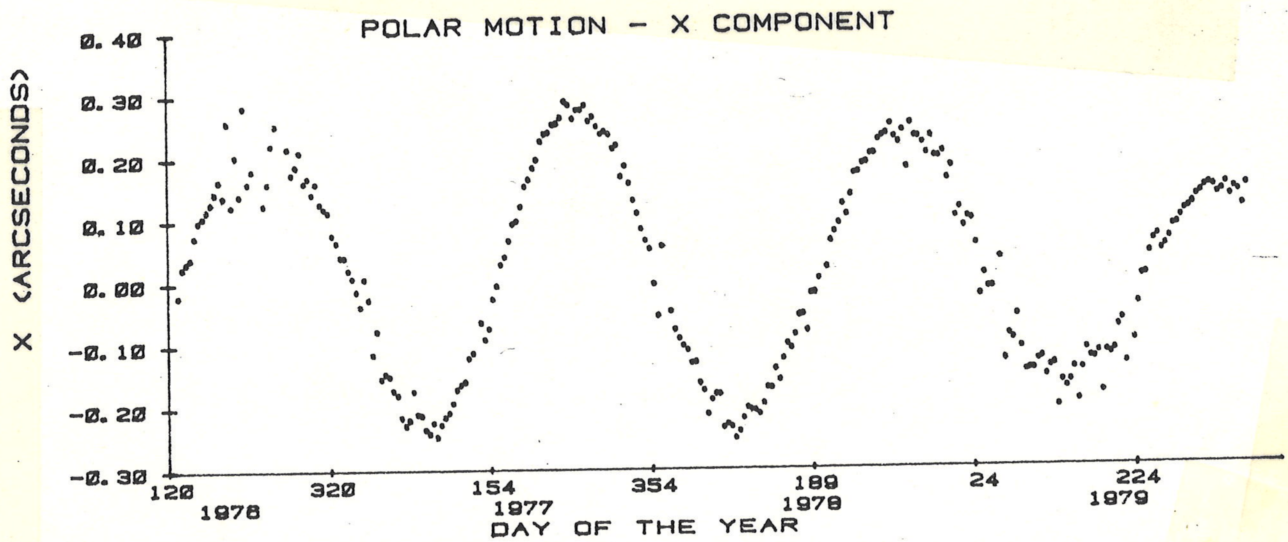

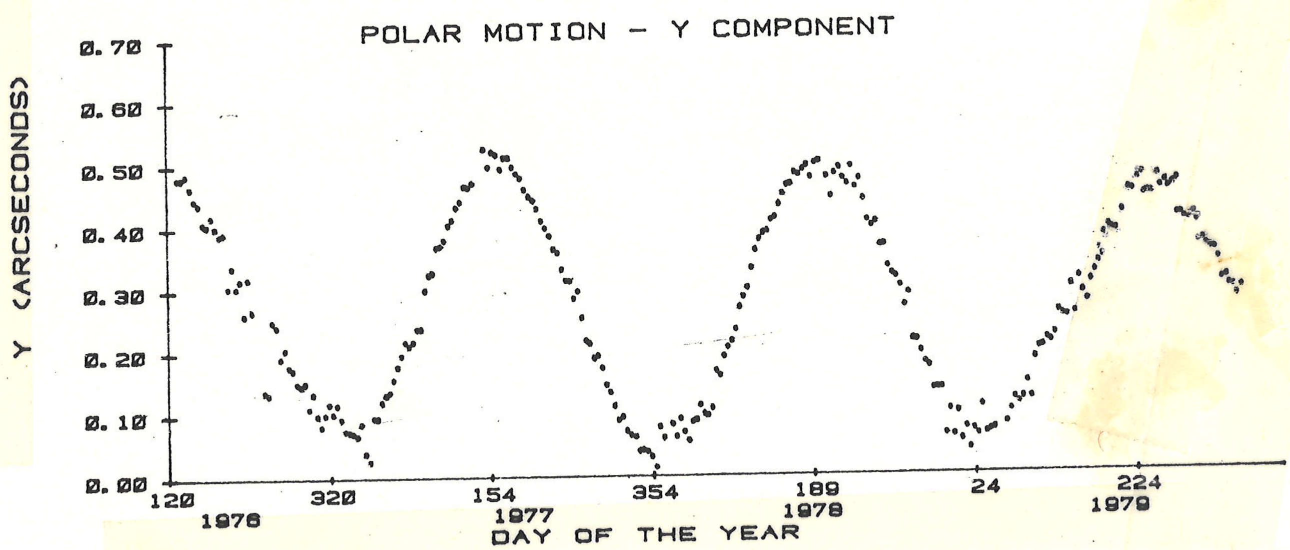

POLE POSITION

From Nov 17, 1983 to Jun 28, 1984
at 5–day intervals
(Circled pts: Y=BIH value)

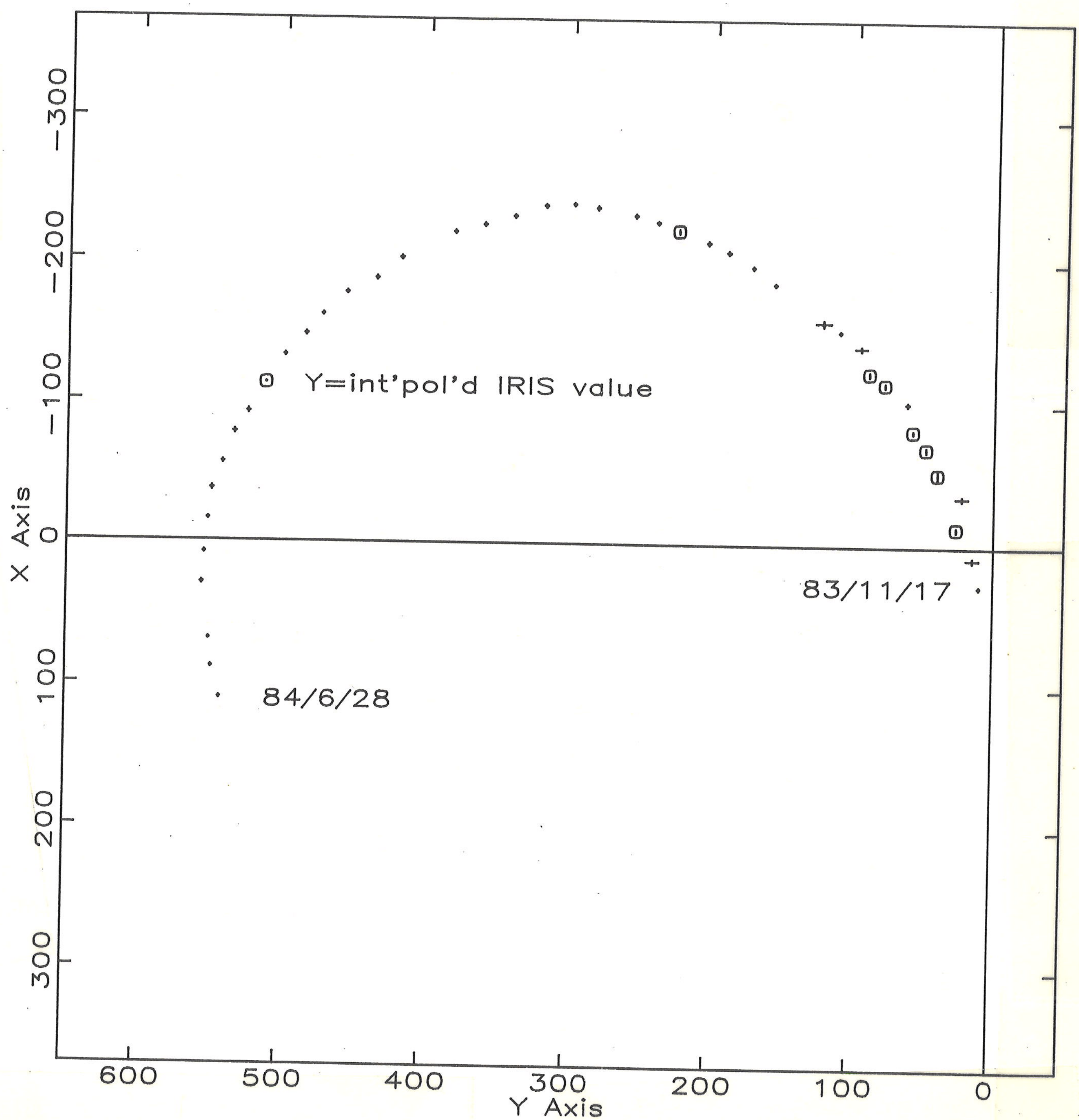

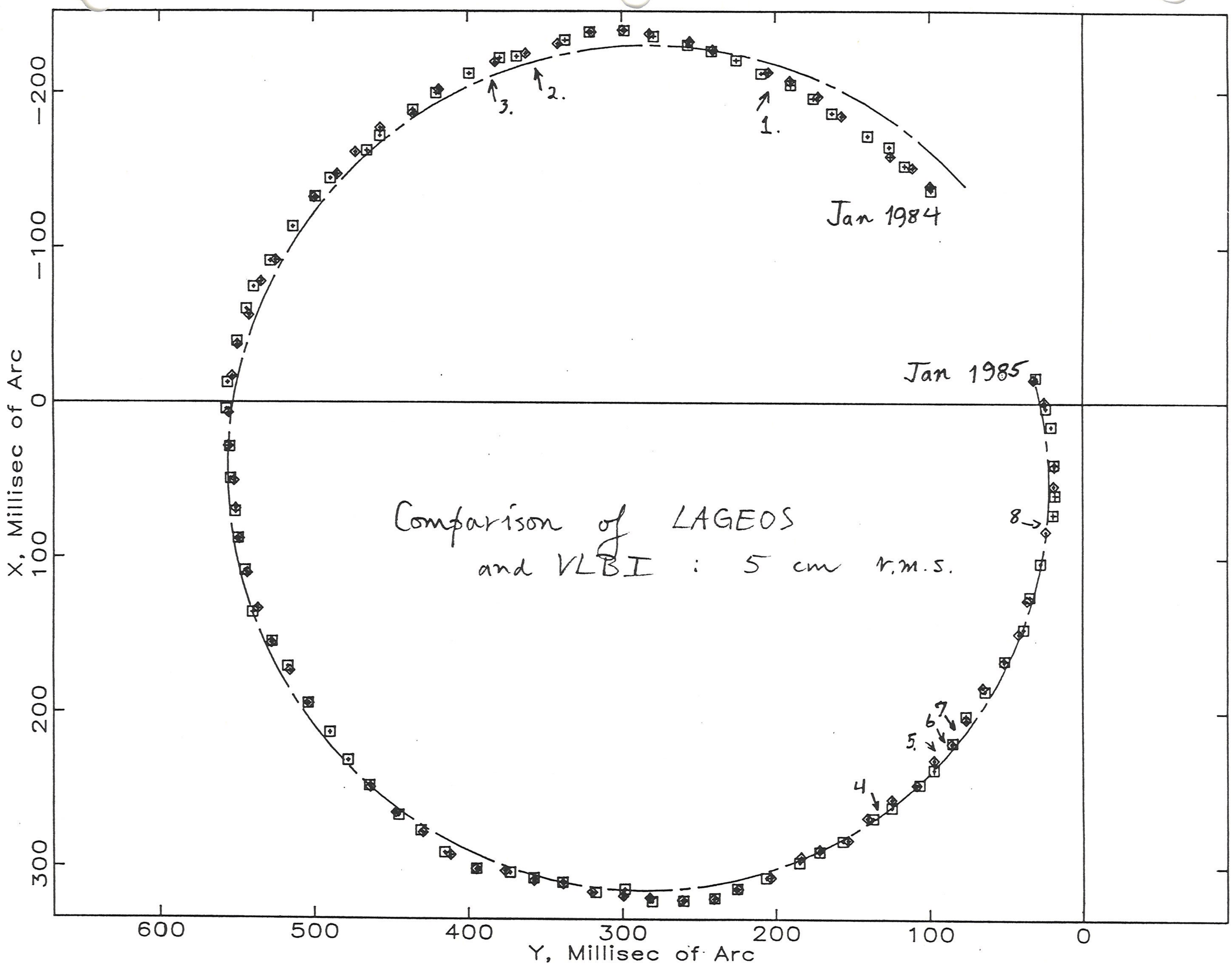
Comparison of LAGEOS and VLBI : 5 cm r.m.s.
Jan 1984
Jan 1985
1.
2.
3.
4
5.
6
7
8
X, Millisec of Arc
Y, Millisec of Arc
-200
-100
0
100
200
300
600
500
400
300
200
100
0

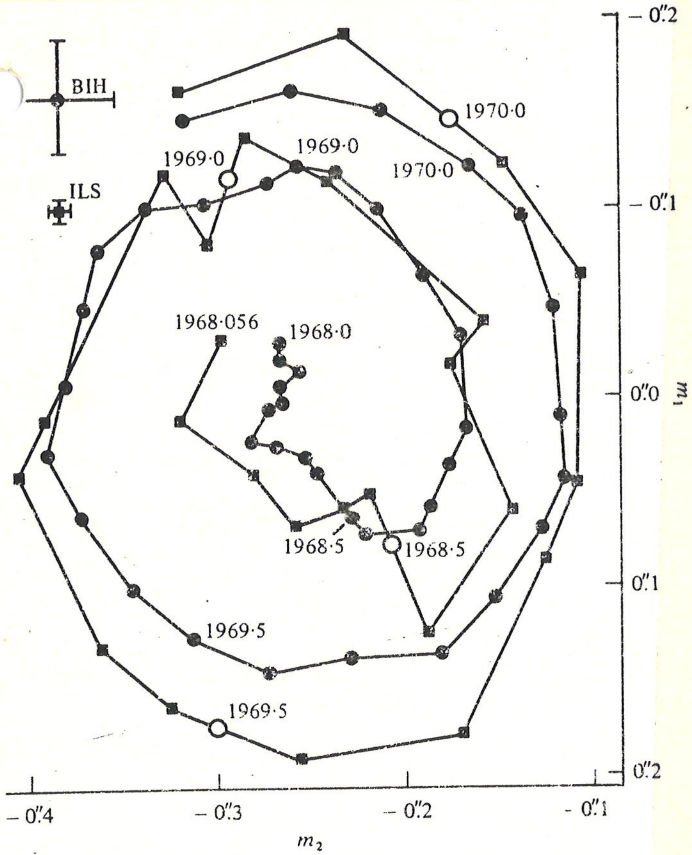

Fig. 5.10. Pole paths as determined by the ILS (■) and by the BIH (●) from 1968.0 to 1970.0. The ILS data are the unsmoothed values given at successive intervals of 0.0833 yr. For convenience in comparing with the BIH results, interpolated values at intervals of 0.5 yr are also indicated. BIH values are the unsmoothed values at intervals of 0.05 yr. Error estimates for the two data sets are indicated at top left-hand side.

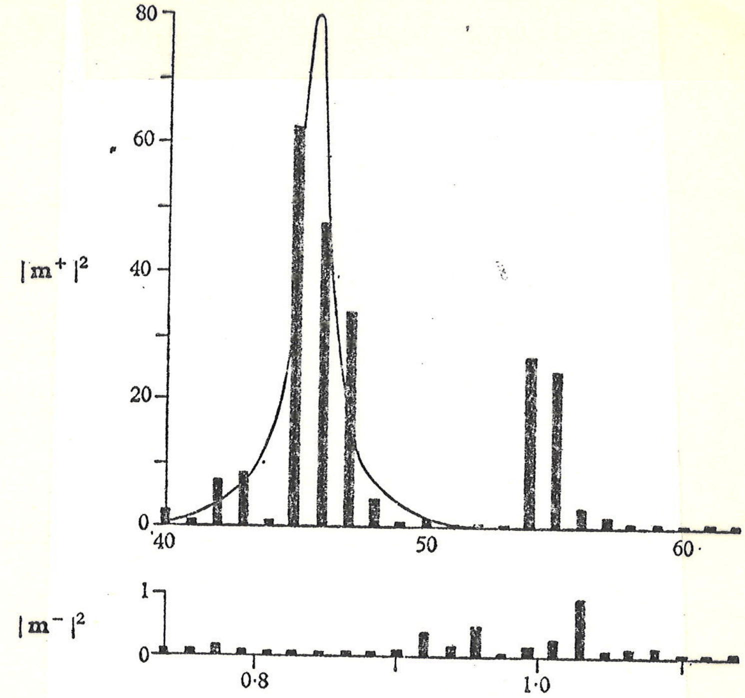

Fig. 7.5. The spectrum of variation in latitude, according to Rudnick (1956). The upper figure refers to the positive (west-to-east) motion, the lower figure to the negative motion of the pole of rotation (see § 6.7). For both motions the harmonics 40 to 62 are shown, with the corresponding frequency scale, in cycles per year, indicated below. The length of the spectral lines gives the contribution per harmonic toward the mean square radius arm (in units of (0″.01)²). The scale for negative motion is ten times that for positive motion. The curve has been fitted by the method of maximum likelihood (see Appendix A.2).

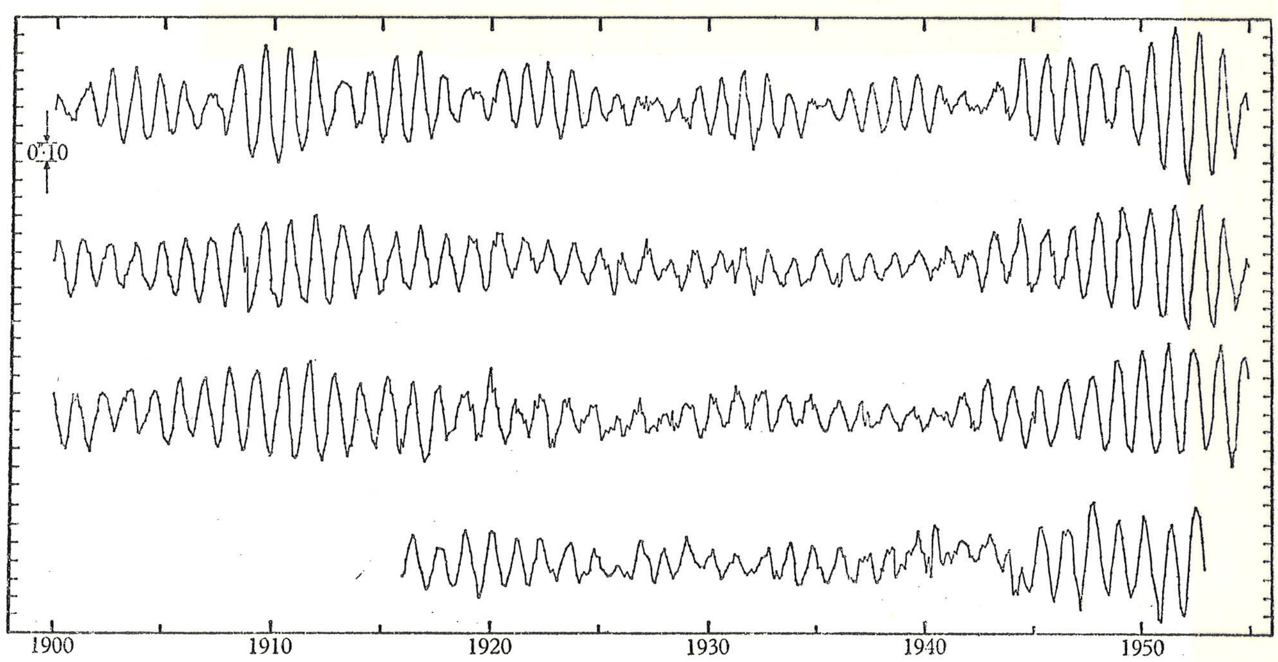

Fig. 7.4. The component, m_1, of the unsmoothed ILS observations, before (*top*) and after (second curve) removal of the seasonal variation; the component, $-m_2$, of the unsmoothed ILS observation after removal of the seasonal variation (third curve) and the corresponding non-seasonal variation in the latitude of Washington, as obtained with the PZT (*bottom*).

<u>Spectrum</u> of wobble looks like:

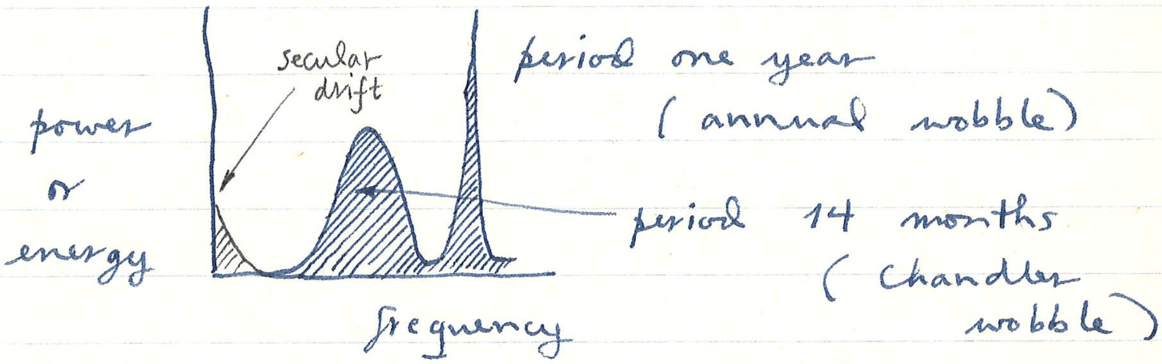

Chandler wobble ~ 75 % of total power
both counterclockwise

Annual wobble is a <u>forced</u> oscillation driven by annual shifts in mass of atmosphere.

High pressure area over Siberia in winter, low in summer, a major atmospheric phenomenon, responsible for <u>monsoon</u> climate of SE Asia, an annual shift in <u>mass</u> of atmosphere from N to S hemisphere <u>forces</u> a shift in solid ⊕ to conserve angular momentum, keep $\underline{H}_\oplus$ in fixed direction.

First quantitative discussion of annual wobble 1916 Sir Harold Jeffreys, allowed for response of oceans to shifting highs and lows by <u>inverted barometer response</u>, integrate only over land.

Hydrological factors also play a role, precipitation, melting of snow + ice etc.

Jeffreys considered also <u>sap rising in trees</u>, leaves on branches, almost but not <u>quite</u> significant.

Agreement of astronomy with meteorology + hydrology is fair considering difficulties of estimating latter. Both <u>amplitude</u> and <u>phase</u> of annual line in fair agreement. See Fig. 4 of Wilson and Haubrich.

~~The 14 month C.W. is a <u>free oscillation</u> of E. Its period now pretty well understood, its energy source or excitation still enigmatic. Will discuss C.W. in greater detail.~~

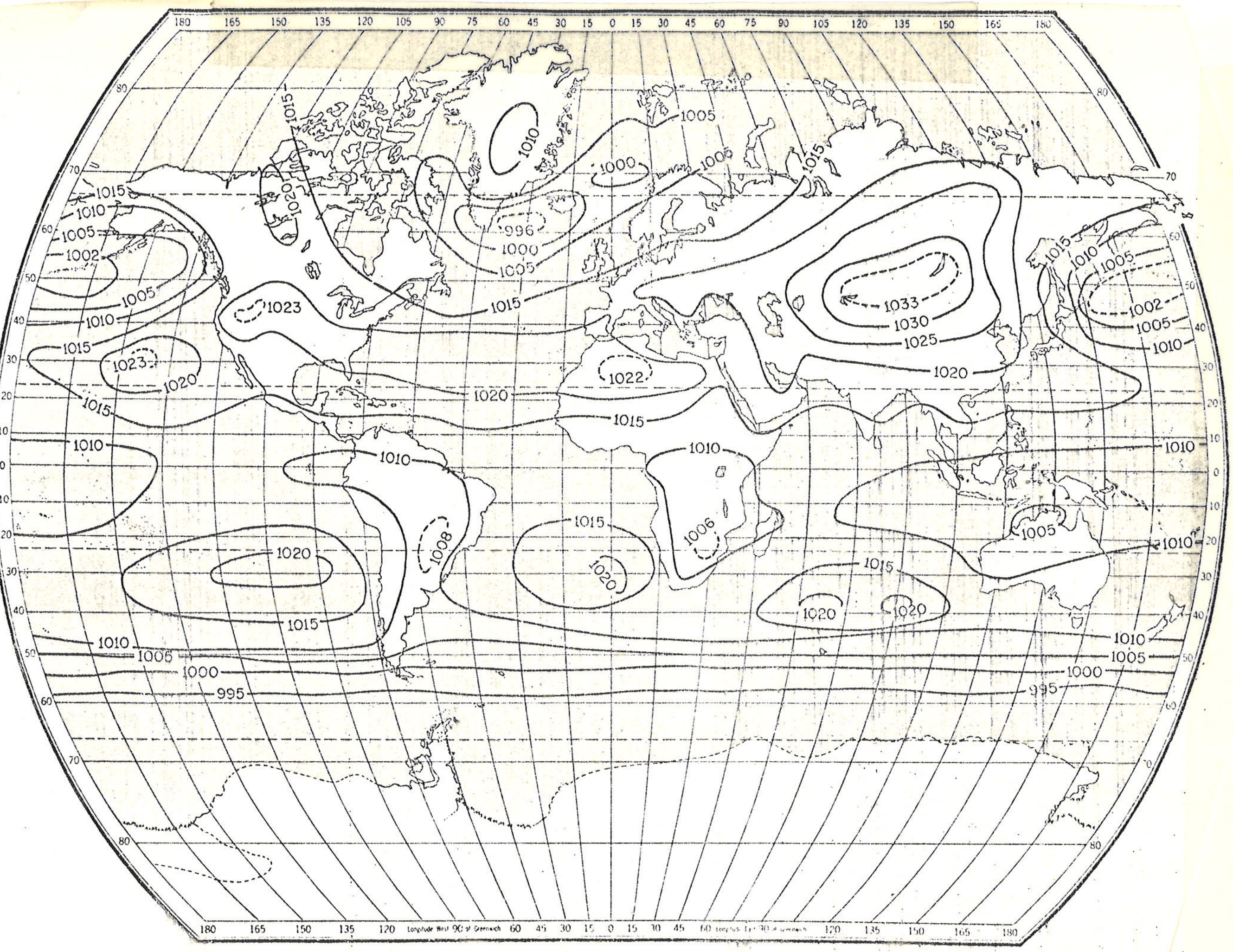

Van der Grinten projection, courtesy A. J. Nystrom & Co., Chicago.

Fig. 4-5 World distribution of mean sea level pressure in January.

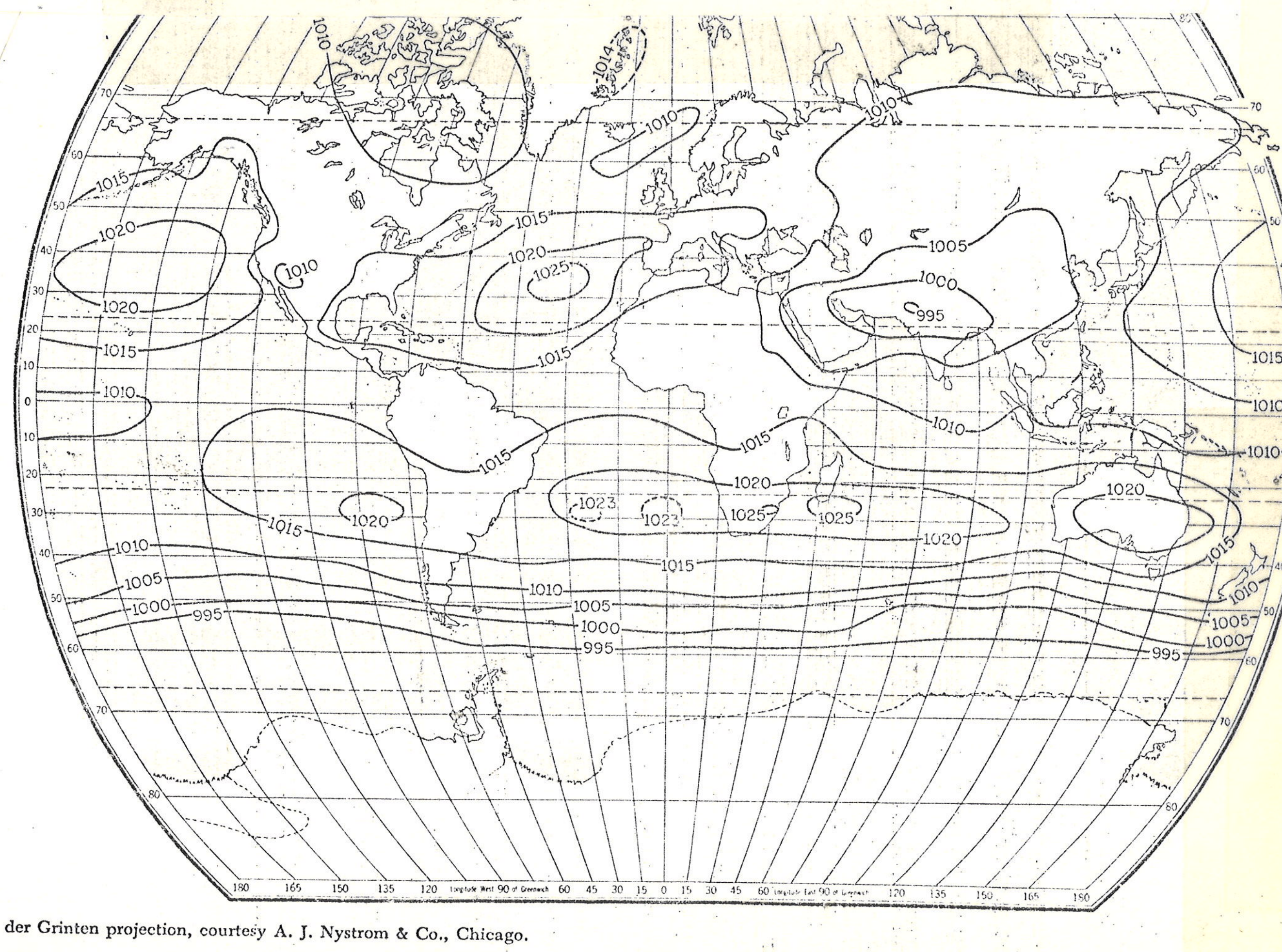

Van der Grinten projection, courtesy A. J. Nystrom & Co., Chicago.

Fig. 4-6 World distribution of mean sea level pressure in July.

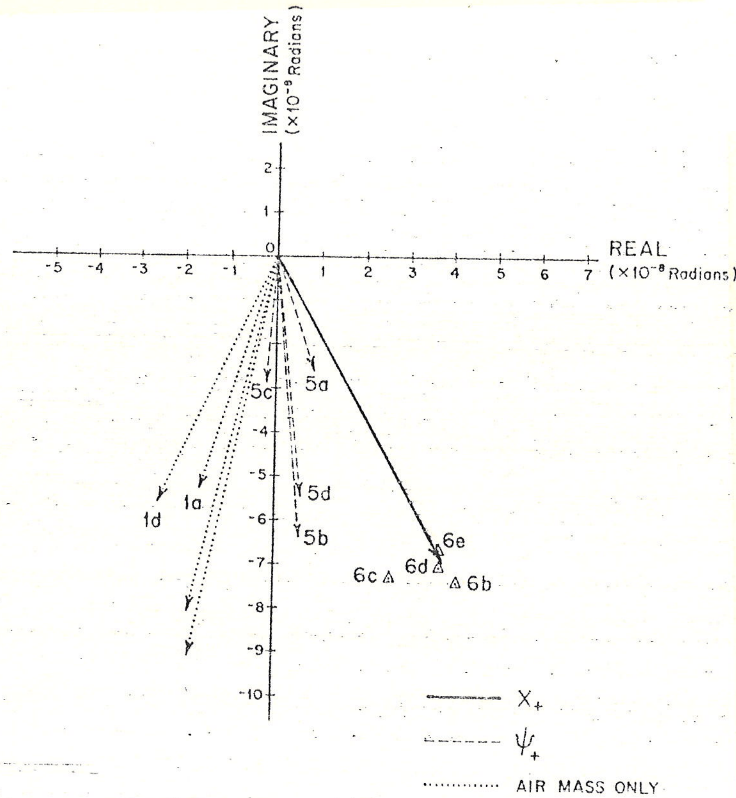

FIG. 4. Positive annual frequency excitations.

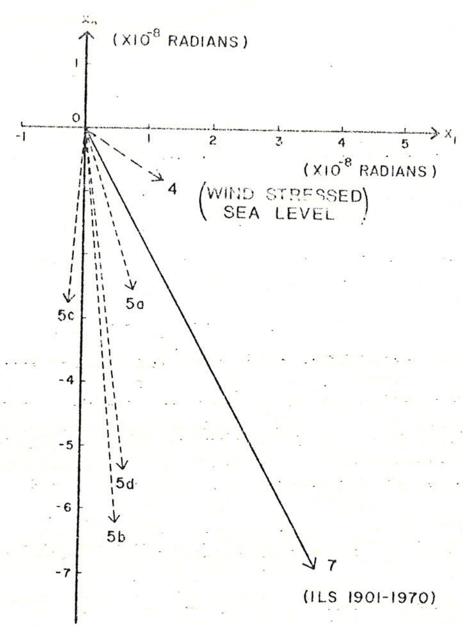

Figure 4. Positive circular annual excitation vector from geophysical estimates of air mass redistribution, continental water storage, and mountain torque (Wilson & Haubrich 1976a, Fig. 4), ILS data and the wind stressed sea level (this study). Numbers refer to lines in Table 3.

Points labelled 1 : shifts in air mass alone.

5 : air mass + hydrological factors gives better agreement with 6 (astronomy)

Fig. 4 from O'Connor shows 4: additional contribution due to simple model of non-isostatic oceanic response to winds, improves agreement when added to 5.

There has also been a secular shift of mean pole since observations began ~ 1900

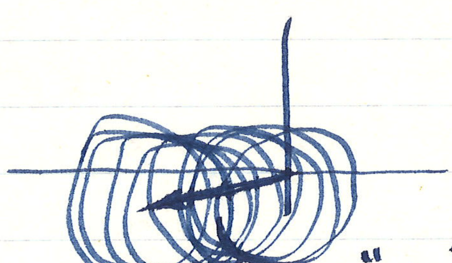

"drift" of center of annual and Chandler wobbles

25 feet ~ 8m

Amount ~ 0.25" in 70 years or about 0".003 /yr toward Labrador, roughly.

10 cm/yr.

3/10 foot / year

This corresponds to a polar wander of about 0.8° per million years which agrees with the observed rate from paleomagnetic data using Jason's hot spot reconstruction.

This supports idea that observed secular drift in ILS data is just recent measurement of same long-term polar wander which has prevailed for last several m.y.

Also has been suggested that it's due to Pleistocene deglaciation – it's certainly in right direction, as figure from Sabadini and Peltier shows

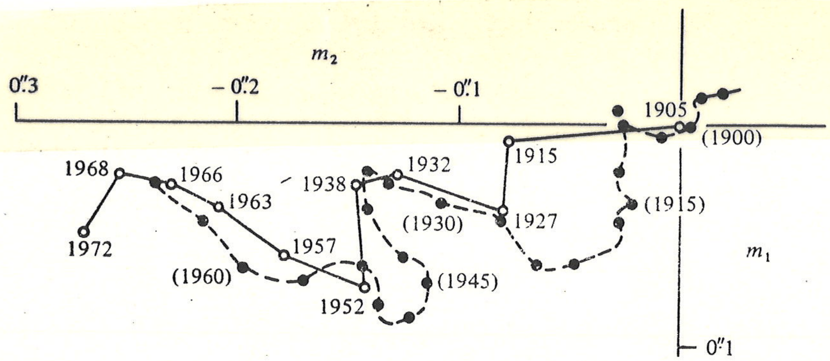

Figure 5.12. Motion of the mean pole according to Stoyko (●, dates in parentheses). Pole positions represent running means based on 6-yr intervals. Positions every 3 yr are indicated. The motion of the mean pole according to Markowitz is indicated by ○; these positions also represent 6-yr means.